Pergamon

Int. J. Solids Structures Vol. 35, No. 19, pp. 2523–2536, 1998

0020-7683/98 $19.00 + .00

PII: S0020-7683(97)00148-0

TENSILE STRENGTH OF TITANIUM MATRIX COMPOSITES: DIRECT NUMERICAL SIMULATIONS AND ANALYTIC MODELS

G. C. FOSTER, M. IBNABDELJALIL and W. A. CURTIN
Department of Engineering Science and Mechanics, Virginia Polytechnic Institute and State University, Blacksburg, VA 24061, U.S.A.
E-mail: curtinw@vt.edu

(*Received* 19 *May* 1997)

Abstract—A recently-developed model for the numerical simulation of tensile stress–strain behavior in fiber-reinforced composites is used to predict the tensile strength of a metal matrix composite consisting of a Ti-1100 matrix reinforced with SCS-6 SiC fibers. Data on the as-processed fiber strengths, interfacial strength, composite size, and fiber volume fraction from Gundel and Wawner are used as input. The predicted strengths agree very well with the sample-specific values measured by Gundel and Wawner, demonstrating the accuracy of the computational model. The effects of free surfaces in a thin ply lay-up geometry are simulated as well, and show a small and surprising increased tensile strength. A modified Batdorf-type analytic model is developed which yields predictions similar to the simulated strengths for the Ti-1100 materials. The ideas and predictions of the Batdorf-type model, which is essentially an approximation to the simulation model, are then compared in more detail to the simulation-based model to more generally assess the accuracy of the Batdorf model in predicting tensile strength and notch strength vs composite size and fiber Weibull modulus. The study shows the Batdorf model to be accurate for tensile strength at high Weibull moduli and to capture general trends well, but it is not quantitatively accurate over the full range of material parameters encountered in various fiber composite systems.

1. INTRODUCTION

Fiber-reinforced composites based on ceramic and metal matrix materials are being developed for a wide array of applications because of their high specific stiffness and strength, and elevated temperature capabilities. One important engineering design parameter is clearly the composite tensile strength in the direction of the fiber loading. It is thus of considerable interest to understand the details of the deformation and failure of these engineered materials at the micromechanical level. Work over the last decade has clearly identified the general mechanism of tensile failure: the accumulation of individual fiber breaks until a "critical" amount of damage is formed which precipitates failure. A model of fiber damage accumulation based on the global load sharing (GLS) concept, wherein broken fibers transfer load equally to all unbroken fibers in the remaining cross-section, has been fairly successful in predicting the tensile strength (Curtin, 1991; MacKay *et al.*, 1991; Weber *et al.*, 1996). The model also clearly demonstrates the role played by various micromechanical factors and constituent material properties such as *in situ* fiber strength, fiber diameter, interfacial sliding resistance, matrix yield stress, and residual stresses (Curtin, 1991). Recent extensions of this model predict the deformation and damage accumulation due to matrix creep and due to explicit fiber strength degradation with time (Fabeny and Curtin, 1996; Du and McMeeking, 1995; Iyengar and Curtin, 1997).

The GLS model has several important (related) limitations because there are no local stress concentrations taken into account. First, the predictions are an upper limit to composite strength and failure is predicted to occur when the tangent modulus reaches zero, which is not observed in practice. Second, the composite strength is not predicted to depend on composite volume, so the difference in strength between coupons and large components cannot be studied. Third, there is no information on material reliability or

failure probability. Fourth, the model cannot predict the effects of notches or of local concentrated damage.

The limitations of the GLS model have motivated the very recent development of more sophisticated local load sharing models which incorporate local stress concentrations during the damage evolution (Zhou and Curtin, 1995; Ibnabdeljalil and Curtin, 1997a; Cox *et al.*, 1994; Xu *et al.*, 1995; Beyerlein and Phoenix, 1997). Because of the extreme increase in complexity of the damage and failure process under LLS, the new models are necessarily based on numerical simulation techniques. The LLS model developed by Curtin and co-workers follows directly from the GLS ideas, but rectifies most of the limitations of the GLS model, although a precise prescription for the degree of load sharing and its dependence on micromechanical parameters has not been provided (Zhou and Curtin, 1995; Ibnabdeljalil and Curtin, 1997a). Preliminary applications of the model to both ceramic and metal matrix composites suggest improved predictions of the tensile strength, including the important size effects (Ibnabdeljalil and Curtin, 1997a).

In this paper, we apply the LLS simulation model in considerable detail to predict strengths of Ti-1100 metal matrix composites, an investigation made possible by the recent careful work on these materials by Gundel and Wawner (1997). Direct numerical simulation of coupon-size specimens yields predicted strengths in excellent agreement with the measured values, and exhibiting trends found in the experimental data. The differences between LLS and GLS predictions are still fairly small, but this is partly due to the small composite sizes tested here. Component-size specimens should exhibit lower strengths, which will be accounted for to some extent by the LLS model, but are absent in the GLS model.

We then return to some analytic concepts developed by Batdorf to form an analytic model which incorporates some but not all of the features of local load sharing simulation model (Batdorf, 1982). For the specific materials tested here, the modified Batdorf model yields predictions very similar to those obtained via simulation, suggesting that the model can provide some insight into the dominant factors in the damage accumulation problem. To investigate the more general utility of the Batdorf model, we then perform a detailed comparison of the predicted scaling of strength with composite volume and of the notch strength vs notch size between the Batdorf model and analytic models based on the LLS simulations and recently developed by two of us. The results show that the Batdorf model predicts tensile and notch strengths quite well for higher Weibull moduli, $m > 10$, which is the range for the experiments discussed here. However, for lower Weibull moduli the Batdorf predictions are much less accurate, which is traced particularly to the absence of a fiber pullout contribution to the strength in that model. These results show that the LLS-based analytic models are preferable to the Batdorf model in most cases (Ibnabdeljalil and Curtin, 1997a; Ibnabdeljalil and Curtin, 1997b).

The remainder of this paper is as follows. In Section 2 we discuss the composite model for metal matrix composites and briefly review the LLS simulation model. In Section 3, we compare predictions of the LLS model to experimental data. In Section 4, we describe the modified Batdorf model and its predictions for the Ti-1100 MMCs. In Section 5 we compare the Batdorf model to the LLS model results. Section 6 contains discussion and a summary of our results.

2. MODEL OF THE COMPOSITE

The composite consists of a volume fraction f of aligned fibers of radius r embedded in an elastic/perfectly-plastic matrix of yield stress σ_y. The fibers have a statistical strength distribution, due to flaws along their lengths, such that the cumulative probability of fiber failure $P_f(\sigma, L)$ in a length L at stress σ is given by the Weibull form

$$P_f(\sigma, L) = 1 - e^{-\frac{L}{L_0}\left(\frac{\sigma}{\sigma_0}\right)^m} \tag{1}$$

where σ_0 is the characteristic fiber strength at gauge length L_0 and m is the "Weibull modulus" describing the variation in fiber strengths. Under an applied tensile load σ, the

first nonlinear event is matrix yielding. Beyond the matrix yield point, which is strongly influenced by residual stresses, the fibers must then carry all of the remaining load so that

$$\sigma = f\sigma_f + (1-f)\sigma_y \tag{2}$$

where σ_f is the load carried by the fiber bundle. Loading beyond the yield point leads to individual fiber breaks at the weaker flaws along the fiber lengths. After a fiber failure, the fiber/matrix interface debonds and the fiber slides with sliding resistance τ against the matrix. The stress in the broken fiber thus recovers from zero back to the far-field load σ_f over a slip length $l_s = r\sigma_f/2\tau$. The load dropped by a broken fiber along the slip length is transferred to unbroken fibers in the local vicinity of the break, increasing the load on the surviving fibers. As the loading increases and damage progresses, local clusters of fiber breaks form which grow larger due to load transfer to the neighborhood. At some critical stress σ_f^*, one such cluster grows continuously outward until the entire specimen is failed. The composite ultimate tensile strength (UTS) is then

$$\sigma_u = f\sigma_f^* + (1-f)\sigma_y. \tag{3}$$

Under global load sharing, where there are no local stress concentrations, it has been shown that a characteristic fiber strength σ_c and gauge length δ_c arise (Curtin, 1991), given by

$$\sigma_c = \left(\frac{\sigma_0^m \tau L_0}{r}\right)^{\frac{1}{m+1}} \qquad \delta_c = \left(\frac{\sigma_0 r L_0^{1/m}}{\tau}\right)^{\frac{m}{m+1}}. \tag{4}$$

Physically, σ_c is the characteristic fiber strength at a length δ_c while δ_c is, in turn, twice the slip length at an applied stress of σ_c. The critical fiber bundle stress σ_f^* is directly proportional to σ_c, and the distribution of fiber lengths protruding from the fracture surface (fiber "pullout") is directly proportional to δ_c. For the Weibull moduli arising in the present work ($m \geqslant 5$), a simple but accurate analytic result for the UTS has been given by Curtin and Zhou (1995):

$$\sigma_u = f\sigma_c \left(\frac{m}{2}\right)^{\frac{m}{m+1}} [1 - e^{(-2/m)}] + (1-f)\sigma_y. \tag{5}$$

An exact result for the GLS problem has been developed recently by Phoenix *et al.* (1997) which is not compactly described, however.

To follow the evolution of fiber damage under LLS, where broken fibers transfer stress only to nearby unbroken fibers, Zhou and Curtin (1995) and Ibnabdeljalil and Curtin (1997a) have developed a numerical simulation model. The model represents each fiber as a string of individual springs, and the fibers are coupled to each other through orthogonal shear springs which serve to transfer load when a fiber breaks. The statistical distribution of fiber strengths is appropriately introduced as the strength distribution of the individual springs, and the fiber slippage along a fiber after breaking is directly included. The load transfer occurs naturally due to the shear springs, and a Green's function technique is used to efficiently accomplish the numerically-demanding process of transferring all of the stress in a manner that is consistent with the spatially-distributed array of fiber breaks that arises during loading of the composite. In the present model, the fibers are arranged in a regular square array. The load transfer is identical to that derived by Hedgepeth and van Dyke (1967) in their classic work, such that a single broken fiber transfers 14.5% of its load to its four neighbors, 6% to its four corner neighbors, and lesser amounts to more distant neighbors. Clusters of broken fibers naturally lead to a build up in stress concentrations on the surrounding fibers, as demonstrated clearly in previous papers.

The simulation model starts with a completely undamaged array of fibers. As the applied load is increased, fiber breaks and associated slip occur, and the stresses are transferred to other fibers. The other fibers may break under the higher loads, and then transfer their loads onto yet other unbroken fibers. Mechanical equilibrium is established when the local loads on each fiber (applied plus transferred) are less than the local fiber strengths. At some critical applied load, however, mechanical equilibrium can never be established as all of the fibers break at least once within a slip-length of some cross-sectional plane along which the composite separates into two pieces. Since the matrix tensile load bearing capacity and the fiber volume fraction are implicit in the numerical model, the output of the model is a specific value for fiber bundle strength σ_f^*. In LLS, it proves convenient to use the characteristic strength σ_c arising in GLS as a normalizing parameter for strengths. The fiber bundle strength depends on both the specific initial distribution of fiber strengths in the tested composite and the physical size (length and number of fibers) in the composite.

In Ti-MMC systems, the samples tested are usually thin specimens fabricated by pressing together single-fiber ply lamina to form a laminate that is only a few fiber diameters in thickness. The fibers on the specimen surfaces thus have fewer neighbors than fibers inside the specimen, and so the load transfer from fiber breaks on the edge is necessarily different from that in a bulk material. Previous LLS simulations have utilized large square sample shapes (e.g. 20×20 or 30×30 fibers) with periodic boundary conditions to simulate large surface-free samples. To directly simulate the thin Ti-MMC specimens commonly tested, we consider here two specialized geometries. First, we consider a thin strip of width four fibers and periodic boundary conditions, so that a broken fiber sees the periodic image of itself four fiber diameters away. Second, we create a thin strip of width four fibers with essentially free surfaces, so that the surface fibers only have three neighbors. This is accomplished by starting with a specimen having a width of eight fibers and periodic boundary conditions, and then artificially breaking exactly one-half of the fibers along their entire length, to create a width of four undamaged fibers and four fibers "removed". Loads are then applied only to the remaining undamaged fibers in the composite to mimic a four fiber width specimen with free surfaces. The load transfer from surface fibers follows directly from the mechanics used in the bulk material, and is not an adjustable parameter. A broken fiber on the specimen surface transfers about 18% of its load to its two surface neighbors and 17% to its interior neighbor, with lesser loads to the more distant fibers; the surface thus causes higher stress concentrations, but on fewer fibers. The output from such simulations is again a value of σ_f^* for the fiber bundle in a thin-strip, free-surface geometry.

3. RESULTS

Gundel and Wawner (1997) have recently presented a very detailed study of the properties of Ti-1100 matrix material reinforced with SCS-6 SiC fibers. Gundel and Wawner prepared panels of varying fiber volume fraction. They then painstakingly extracted fibers from as-processed coupons and performed single fiber tensile tests to determine the fiber strength distribution in each panel. The *in situ*, or post-processed, fiber strengths showed some deviations from the pristine fiber strengths and, more importantly, showed substantial panel-to-panel variations that have a marked influence on the composite tensile strength. Most of the panels showed strength distributions following a Weibull distribution, and the characteristic strength σ_0 measured at a gauge length $L_0 = 1''$ and Weibull modulus m for the different panels are shown in Table 1.

Gundel *et al.* also performed fiber pushout tests on individual fibers in each set of panels to obtain the interfacial sliding resistance τ, shown in Table 1. Although the pushout test geometry and loading are not identical to the situation around an internal fiber break, pushout-derived sliding resistances follow the trends measured by other techniques and so we consider them fairly reliable. The sensitivity of the strength predictions to τ is also not too strong. The matrix yield stress was determined to be $\sigma_y = 935$ MPa. Finally, Gundel and Wawner performed tensile tests on coupons from each of these panels, using specimens containing essentially a fixed number of fibers and a gauge length of 1.5". The average

Table 1. Measured constitutive properties of Ti-1100 MMC materials, and calculated values of the characteristic strength σ_c and length δ_c

Sample	f	m	σ_0 (MPa)	τ (MPa)	σ_c (MPa)	δ_c (mm)
B	0.15	10.1	3930	188	5082	1.892
C	0.18	13.9	4310	≈190	5191	1.913
D	0.20	5.8	2890	190	4608	1.698
F	0.26	12.3	4270	≈65	4856	5.229
G	0.28	12.6	4640	≈65	5229	5.632
H	0.30	6.8	3330	65	4280	4.609
I	0.35	11.6	4410	81	5126	4.430

strengths for coupons from each panel are shown in Table 2. Samples A and E of (Gundel and Wawner, 1997) are not shown in Tables 1 and 2 because these samples displayed a bimodal fiber strength distribution and so did not neatly fit into most analytic models. However, provided the relative populations of high and low strength fibers are available, the simulation model could be easily extended to handle multiple fiber strength distributions.

With the above detailed information on specific specimens, we have used the numerical LLS simulation model to predict the tensile strengths of each set of specimens. The inputs to the theory are the fiber strength distribution (σ_0, m at L_0), interfacial sliding τ, and fiber radius of $r = 70$ μm which are used to determine the normalizing parameters σ_c and δ_c via eqn (4), shown in Table 1. We also use 104 fibers of length 1.5″ in a thin strip geometry of 4×26 fibers, which closely approximates the dimensions of the specimens tested. We are thus essentially directly simulating the physical composites tested in the laboratory by Gundel and Wawner (1997). The output of the simulation model is a value for the bundle strength σ_f^*, which is then combined with the volume fraction f and σ_y in eqn (3) to obtain the composite UTS.

Results of the simulated tensile strengths are shown in Table 2 and Fig. 1. The agreement between measured and predicted strengths on specific samples is excellent, typically being within 10%. The predicted values also follow some of the observed trends. For instance, sample D has a strength comparable to sample B in spite of a larger fiber fraction because of its anomalously low fiber strengths and Weibull modulus. For comparison, two other strength predictions are shown in Table 2 and Fig. 1: the GLS value from eqn (5); and the rule-of-mixtures (ROM) obtained by simply replacing σ_f^* with the measured σ_0 in eqn (3). The GLS value is always larger than the LLS value, and so agrees less well with the data; the differences between LLS and GLS are not too large here, however, because of the fairly small physical coupon size tested. The ROM strengths are generally even larger than the GLS predictions and are typically 100–200 MPa larger than the LLS predictions, and are also independent of composite size. The relative differences between models appear small in part because of the large contribution of the matrix to the composite strength in all cases. While all three models follow the general trends, the LLS model consistently narrows the difference between theory and experiment in all cases.

Table 2. Composite tensile strengths (in MPa) for Ti-1100 MMCs as measured and as predicted by the LLS model (periodic and free-edge), GLS model, rule-of-mixtures, and Batdorf-type model. Also shown are the predicted average fiber pullout lengths as predicted by the LLS model

Sample	Measured	LLS (periodic)	LLS (free-edge)	GLS	ROM	Batdorf	LLS pullout (μm)
B	1252	1341	1348	1392	1384	1334	210
C	1300	1470	1474	1531	1543	1464	220
D	1230	1353	1367	1414	1326	1319	190
F	1496	1630	1643	1708	1802	1631	600
G	1724	1768	1789	1856	1972	1766	650
H	1327	1535	1546	1605	1654	1502	550
I	1716	1929	1938	2041	2151	1900	510

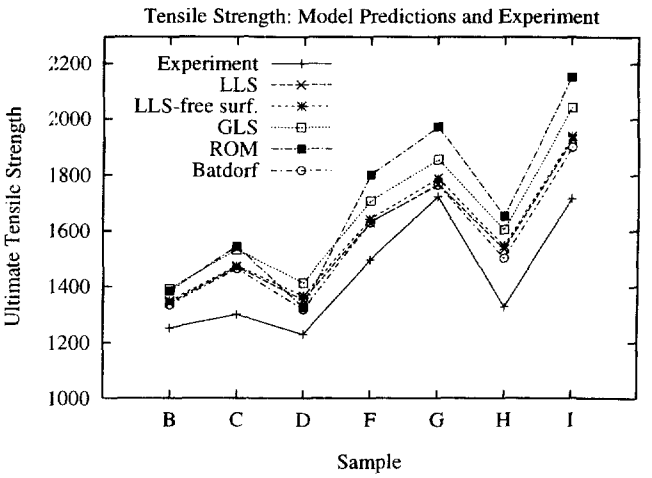

Fig. 1. Ultimate tensile strengths (in MPa) for samples studied here (see Table 2 also), as measured experimentally and predicted by the local load sharing, global load sharing, rule-of-mixtures, and Batdorf-type models, respectively. All predictions generally follow trends in the experimental data, but the LLS and Batdorf models give the best agreement and differ from experiment by only 10% on average.

Interestingly, the influence of free-surface boundaries in a strip geometry is almost negligible. Results for the four-fiber width system with periodic boundaries actually show slightly lower strengths (10–20 MPa) than for the free-surface four fiber width system. Thus, the higher stress concentration on fewer fibers that occurs in the free-edge geometry is slightly beneficial to the strength. Such results cannot be anticipated *a priori*. However, from a design perspective, it is useful to know that the overall ply thickness does not have a detrimental effect on tensile strength even for fairly thin specimens. The use of a square fiber array in the simulations, rather than a hexagonal array, might cause some differences between theory and experiment but those differences are probably not large, in light of the results found here using free-edge specimens.

At the end of the simulation, the plane of separation of the material can be determined and pullout length calculated. In GLS, the average pullout length is predicted to be $\langle L \rangle = \frac{1}{4}\lambda(m)\,\delta_c$ where $\lambda(m)$ depends slowly on m and is around unity. In LLS, $\langle L \rangle$ is still controlled by δ_c but the coefficient λ can differ, and is usually smaller. Taking the values of $\lambda(m)$ from Curtin (1991), the predicted pullout lengths, according to GLS, are ≈ 400 μm for samples B, C, D (high τ) and range from 960 to 1210 μm for samples F, G, H, I (smaller τ). The predicted pullout lengths, according to the LLS simulation (periodic-edges), are ≈ 200 μm for samples B, C, D and range from 510 to 650 μm for samples F, G, H, I. All materials tested exhibited pullout on the order of 200 μm. Thus, there is a discrepancy here for the smaller-τ materials, suggesting fiber fracture is more localized to a plane than predicted. It is not clear whether this is a limitation of the model or due to dynamic effects in the real composites when they undergo rapid failure upon reaching the UTS.

Differences between the present theory and experiment might be traced to a variety of sources. First, the precise value for matrix yield stress is not well-established. Second, the pushout value for τ is approximate. Third, the load sharing used in the theory is that of Hedgepeth and Van Dyke, and does not consider issues specific to the Ti-MMC system. Fourth, initial fiber damage might exist in these materials. Fifth, dynamic fiber fracture and interface damage are not incorporated into the present model. Given the reasonable agreement between theory and experiment, however, these issues may not be significant.

In summary, the LLS simulation model provides accurate predictions of Ti-MMC coupon strengths when the fiber, matrix, and interface constitutive information is well-established. Gundel and Wawner have also shown that these models also predict the nonlinear stress–strain above matrix yielding quite well. These results for strength demonstrate that the LLS model can form the basis for the further development of detailed

predictive models for notch strength, damage tolerance, and time-dependent degradation and durability in Ti-metal matrix composites.

4. AN ANALYTIC BATDORF-TYPE MODEL

Some years ago, Batdorf (1982) proposed a simple cumulative local damage model for predicting failure in unidirectional fiber composites. The Batdorf model followed from some earlier more-detailed asymptotic analyses by Harlow and Phoenix (1981), but was framed in a manner suitable for easy computations. Gundel and Wawner (1997) presented the results of a Batdorf model calculation, but without providing sufficient details to reproduce their results. Here, we follow the Batdorf analysis with a few minor modifications to produce an analytic model corresponding closely to our LLS model for failure. Essentially, our Batdorf model is an approximation to the LLS simulation model. The predictions of the analytic Batdorf model are remarkably close to the LLS results for the present Ti-MMC sample, in spite of the simplifications. However, we show in Section 5 some important limitations of the Batdorf model by making more careful and general comparisons to the LLS results.

The Batdorf model considers damage to occur in the form of isolated compact planar clusters of breaks which grow under increasing applied load due to stress concentrations at the edges of the cluster (Batdorf, 1982). Conceptually, the model calculates: (i) the expected number of single isolated fiber breaks, Q_1, in a volume V under applied stress σ; (ii) the number of isolated breaks which will grow to become a cluster of two breaks at the same stress σ because of stress concentrations on the neighbors of the first break; (iii) the number of two-break clusters which then grow to three-break clusters, and so on. At any fixed stress, the number Q_i of each cluster size i is determined. The typical largest cluster at any applied stress is that size i for which $Q_i \approx 1$, i.e. there is about one cluster of this size in the entire volume. Failure occurs at that stress for which the largest size cluster (some size i^*) will grow with probability unity to size i^*+1 with no increase in applied stress, which will then grow to size i^*+2, and so on until the cluster spans the entire system. Thus, there is a critical point in the theory at which the largest cluster becomes unstable to growth.

The calculation of the number Q_i of i-break clusters (coined i-plets by Batdorf) proceeds as follows. Suppose at stress σ there are Q_i i-plets, each of which has n_i immediate neighbors around its perimeter which are experiencing stress concentrations of c_i in the plane of the breaks. Suppose further that the stress on each neighbor decays linearly, due to slip along the broken fibers, from the value of $c_i\sigma$ to the far-field value σ over some length $\delta_i/2$. Then, the probability of failure of a single neighboring fiber can be found by integrating the Weibull probability of failure over the length experiencing the overstress as

$$p_i = \frac{c_i^{m+1}-1}{(c_i-1)(m+1)}\frac{\delta_i}{L_0}\left(\frac{\sigma}{\sigma_0}\right)^m. \tag{6}$$

Since each neighbor has this probability of failure, the number of Q_{i+1} clusters formed from the Q_i clusters is simply

$$Q_{i-1} = Q_i n_i p_i. \tag{7}$$

The initial starting point for this iterative evolution of break clusters is the number of expected 1-plets in the entire volume of the material,

$$Q_1 = N\left(1-e^{-\frac{L}{L_0}\left(\frac{\sigma}{\sigma_0}\right)^m}\right) \approx N\frac{L}{L_0}\left(\frac{\sigma}{\sigma_0}\right)^m \tag{8}$$

where the approximation is accurate if $Q_1 \ll NL/\delta_1$, which is always the case.

At any stress σ, the above scheme generates a set of $\{Q_i\}$ values. The point of failure is then found as that stress at which there is a cluster size i^* which simultaneously satisfies the conditions

$$Q_{i^*} = 1 \tag{9}$$

$$Q_{i^*+1} > Q_{i^*}. \tag{10}$$

The first condition states that there is typically one cluster of size i^* in the entire system. The second, critical, condition states that the i^* system is actually unstable to growth to size $i^* + 1$ at the current stress. Both conditions are necessary for failure to occur. The stress σ at which failure is calculated from eqn (6)–(10) is precisely the fiber bundle failure stress σ_f^* in eqn (3), and the UTS follows from eqn (3).

To make explicit connection with our simulation results, and the expected mechanics of the debonding and sliding interface in Ti-MMCs, we proceed as follows. First, the fibers are arranged in a square array. The clusters of planar breaks are chosen to be nearly circular and the stress concentration factors for planar clusters of fiber breaks are as obtained from our simulations, which are identical to those given by Hedgepeth and van Dyke (1967). These choices are also identical to those used previously by Batdorf and Ghaffarian (1982), and the relevant values of n_i and c_i are shown in Table 3. Finally, the length $\delta_i/2$ is chosen to be the slip length at the current stress level, independent of the cluster size i, so that

$$\delta_i = \frac{r\sigma}{\tau} = \delta_c\left(\frac{\sigma}{\sigma_c}\right). \tag{11}$$

This condition on δ_i leads to the same slip lengths as used in the LLS simulation model. Substituting this result into eqn (6), and introducing the normalizing parameters σ_c and δ_c for stress and length, respectively, the final result for the number of Q_i breaks clusters at stress σ is given by

$$Q_i = \frac{NL}{\delta_c}\left(\frac{\sigma}{\sigma_c}\right)^{i(m+1)-1} \prod_{j=1}^{i-1} \frac{n_j(c_j^{m+1}-1)}{(c_j-1)(m+1)}, \tag{12}$$

which is obtained by combining eqns (6)–(8). Calculating the Q_i values from eqn (12) and applying the failure conditions of eqns (9)–(10) leads to predictions for the composite strength. With the input of the materials tested by Gundel and Wawner to obtain σ_c and δ_c, the predicted strengths are shown in Table 2 and Fig. 1. Interestingly, the predicted strengths are generally extremely close to those found in the simulation model. In fact, the Batdorf model results are generally very slightly closer to the measured values than the simulation model strengths.

In the two cases with low-m fibers (samples D, H) the Batdorf result is rather lower than the simulation model. This stems from one important difference between the Batdorf and simulation models: the role of fiber pullout. In the Batdorf model, the probability of fiber breakage is calculated based on an overstressed region of $\pm\delta_i/2$, but then the break

Table 3. Number of near neighbors n_i and stress concentration factor c_i on those neighbors, for various clusters of near-circular fiber breaks up to $i = 12$ and for square arrays of fiber breaks of size i for $i > 12$

i	1	2	3	4	5	6	7	8	9	10
c_i	1.146	1.18	1.225	1.281	1.31	1.34	1.375	1.405	1.456	1.46
n_i	4	6	7	8	9	10	11	11	12	13
i	11	12	16	25	36	49	64	81	100	
c_i	1.48	1.5	1.582	1.728	1.841	1.975	2.083	2.2	2.303	
n_i	14	15	16	20	24	28	32	36	40	

itself is placed in the same physical plane as the previous breaks in the cluster. The fibers are, therefore, all broken in the same plane and there is no pullout, or remaining fiber load carrying capability, after a fiber breaks. In the LLS model, the three-dimensional character of the fiber breakage is explicitly included. At higher Weibull moduli, there are shorter pullout lengths and less fiber damage prior to failure, so that the pullout contribution of the broken fibers to the composite strength is small. At lower Weibull moduli, the pullout makes an important contribution to the strength. The absence of pullout in the Batdorf model is, therefore, believed to be responsible for the slightly lower strengths for the low-m material. It is also conceptually inconsistent since the probability of fiber breakage was determined including the possibility of failure well away from the plane of the previous breaks. The Batdorf model does lead to slightly better agreement with experiment in these cases, but this is an artifact of the no-pullout approximation. The pullout observed on the fracture surfaces of the Ti-MMCs is smaller than predicted by the simulation model for the materials with lower τ values, but it is not sensitive to the precise m value.

5. COMPARISON OF BATDORF AND LLS MODELS

Given the very close similarity of the Batdorf and simulation predictions for the Ti-1100 MMC materials, it is worth analyzing more closely the similarities and differences between the two models. The two models use the same fiber geometry, and the stress concentrations for planar arrays of breaks are identical. However, the simulation model accounts for the actual longitudinal location of the fiber breaks, and hence pullout and a smearing of the stress concentration factors; this would tend to increase the predicted strength. The simulation model also distributes stress to further neighbors beyond the immediate perimeter, allowing for more damage and coalescing of damage; this would tend to decrease the predicted strength. The Batdorf model permits just one cluster shape of each size and uses an average stress concentration factor along the perimeter, whereas complex cluster shapes and local stress concentrations arise quite naturally in the simulation model; these suggest lower strengths in the simulation model. In the Batdorf model, the total applied force is not conserved: the total force redistributed from a broken fiber to the neighboring fibers is less than the force on the fiber, which increases the strength prediction. From these points, it is clear that the Batdorf model developed here corresponds to an approximation of the LLS simulation model. To create an analytic model, Batdorf has eliminated certain more-complicated aspects of the failure that are naturally included in the LLS simulation model. In total, however, for small specimen sizes and higher fiber Weibull moduli our results above indicate a remarkable balancing of all of the competing complex factors that are left out of the Batdorf model. The differences between Batdorf and LLS simulation results are also somewhat minimized by the additional strengthening from the matrix itself, which contributes around 700 MPa to the strengths, and makes relative differences appear smaller. Below, we study the size scaling of the two models in more detail to check the general agreement over a range of composite sizes and a broader range of Weibull moduli, and find that important differences do exist between the LLS model and the more-approximate Batdorf model.

5.1. *Size scaling*

An important aspect of any model including local load sharing is the predicted size scaling of strength. Two of us have recently developed an analytic model for the strength scaling under LLS, which is based on a detailed analysis of the numerical simulation results and some fascinating connections between the failure under LLS and GLS conditions (Ibnabdeljalil and Curtin, 1997a). Here, we analyze in more detail the Batdorf model predictions for tensile strength vs composite size and fiber Weibull modulus, and compare them in detail to the analytic LLS model (which yields predictions identical to those obtained in the LLS simulations).

In the LLS analytic model, the composite is conceptually viewed as consisting of a collection of small fiber bundles of length $\delta_l = 0.4\,\delta_c$ and n_l fibers in the cross-section. A

volume of N fibers in a length L thus consists of $\mathcal{M}\mathcal{N}$ small fiber bundles, where $\mathcal{M} = L/\delta_1$ and $\mathcal{N} = N/n_1$. The size n_1 is (empirically) related to the fiber Weibull modulus by

$$n_1(m) = 403m^{-1.28} \quad 2 \leqslant m \leqslant 10. \tag{13}$$

At any fixed size, the strength distribution is found to be a Weibull distribution and the characteristic (Weibull reference) strength of a composite of volume NL is predicted to be

$$\bar{\sigma} = \frac{\tilde{m}\gamma^{**}}{\sqrt{2\log \mathcal{M}\mathcal{N}}}\Gamma\left(1+\frac{1}{\tilde{m}}\right) \tag{14}$$

with a composite Weibull modulus of

$$\tilde{m} = \frac{\mu^*}{\gamma^{**}}\sqrt{2\log \mathcal{M}\mathcal{N}} + \log\left(\frac{2\sqrt{\pi \log \mathcal{M}\mathcal{N}}}{(\mathcal{M}\mathcal{N})^2}\right) \tag{15}$$

where $\Gamma(\cdot)$ is the gamma function and the parameters μ^* and γ^{**} are the strength and its standard deviation, respectively, of a bundle of size n_1 fibers failing under global load sharing, and are tabulated in (Ibnabdeljalil and Curtin, 1997a). This model has been shown to reproduce the LLS simulation results with very high accuracy.

In the Batdorf model, the calculated strength is the characteristic strength as well, but the results are not expressible in a simple analytic form. The central portion of the strength probability distribution is also predicted to be Weibull in form with a Weibull modulus of mi^*, where i^* is the size of the critical cluster of fiber breaks. Determination of the strength and Weibull modulus vs size process by direct calculation from eqns (5)–(8) above after specific input of the size NL.

Figures 2(a–c) show the dimensionless fiber bundle strength σ_f^*/σ_c vs dimensionless composite size (NL/δ_c), as predicted by the Batdorf and LLS models for fiber Weibull moduli of $m = 2$, 5 and 10, respectively. Discontinuities in the Batdorf models arise because neighboring size ranges will have different values for the critical cluster size leading to failure. These artifacts become less pronounced as size is increased or Weibull modulus decreased. Neglecting the discontinuities in the Batdorf predictions, the two models agree on the general trend of behavior. As expected from our previous results, the two models also agree quantitatively for high Weibull moduli. The discrepancies become glaring as m is reduced, however, and for $m = 2$ the Batdorf model severely underestimates the composite strength. Since $m = 2$–5 is a typical range for many fibers, the Batdorf model should not be used in such cases. In spite of the overall differences in magnitude, the predicted scalings of strength with composite size are remarkably similar. The origins of this similarity are not yet understood however. These results suggest the Batdorf model can be used reliably at higher m, $m \geqslant 10$, and over a wide range of sizes.

5.2. *Notch strength*

A second comparison between the Batdorf and simulation models can be made by considering their respective predictions of "notch strength". Ibnabdeljalil and Curtin (1997b) have recently presented simulations of composite failure in the presence of an initial "notch" consisting of a square planar array of broken fibers. Failure around such notches was found to depend on the stress concentration around the notch and the extent of fiber pullout, which is strongly dependent on fiber Weibull modulus. In terms of the notation used here, the normalized notch strength of the composite was found to be

$$\sigma = \frac{\mu^*}{c_i} + \sigma_p \tag{16}$$

where the normalized pullout stress σ_p is given by

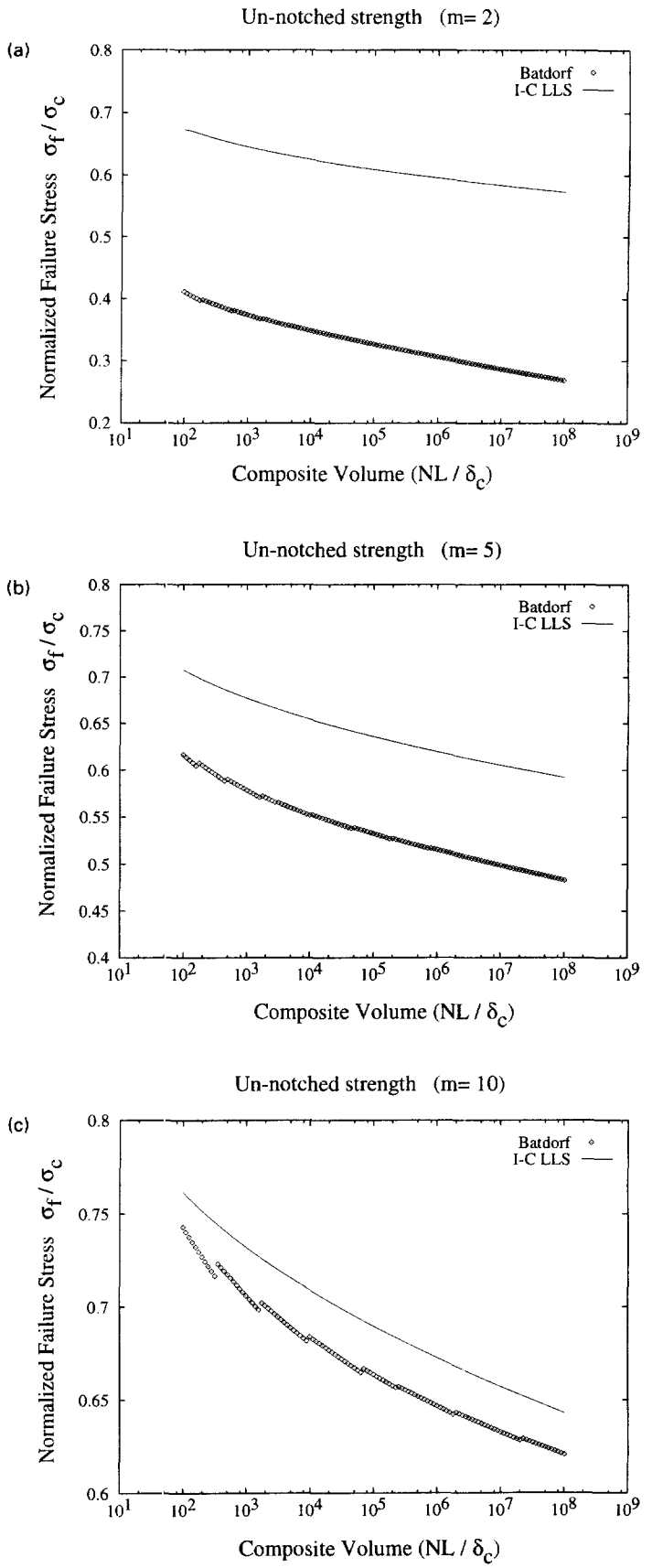

Fig. 2. Normalized fiber bundle strength σ_f^*/σ_c vs normalized composite volume (NL/δ_c) as predicted by the Batdorf-type model and the LLS analytic model of Ibnabdeljalil and Curtin (IC), for fiber Weibull moduli of (a) $m = 2$, (b) $m = 5$, and (c) $m = 10$.

$$\sigma_p = \left(\frac{1}{m+1}\right)^{\frac{m}{m+1}} \Gamma\left(\frac{m+2}{m+1}\right). \tag{17}$$

In the Batdorf-type analysis, an initial notch of size i_n can be introduced by simply setting $Q_{i_n} = 1$ at the outset. Failure due to such an initial notch then occurs when the notch begins to grow unstably, i.e. when $Q_{i_n+1} = 1$. Damage occurring elsewhere in the system evolves separately and need not be considered in this model. From the Batdorf analysis of eqn (7), we see that the failure emanating from an initial notch of size i_n occurs when

$$Q_{i_n} = Q_{i_n+1} = 1 = n_{i_n} p_{i_n}. \tag{18}$$

Solving this condition for the stress yields the notch strength of

$$\sigma_f^* = \left(\frac{(c_{i_n}-1)(m+1)}{n_{i_n}(c_{i_n}^{m+1}-1)}\right)^{\frac{1}{m+1}}. \tag{19}$$

The required values of n_{i_n} and c_{i_n} for large notches are not contained in (Batdorf, 1982) and (Batdorf and Ghaffarian, 1982). However, for square notches of size i_n, the maximum stress concentration factors have been calculated in (Ibnabdeljalil and Curtin, 1997b) and are also shown in Table 3. The number of near neighbors n_i is taken simply as $4n_i$, which neglects the neighbors on the corners of the square notch.

The predicted notch strengths from the Batdorf and LLS models are shown in Fig. 3 for Weibull moduli of $m = 5$ and 10. For $m = 10$, the model predictions are nearly parallel, with a modest (10%) difference in magnitude. For $m = 5$, however, there is a much larger difference in the predicted behaviors. The Batdorf model predicts a much more rapid weakening of the notch strength with increasing notch size than predicted by the LLS model or seen in the LLS simulations. Furthermore, the Batdorf model predicts that the $m = 5$ strengths are always below the $m = 10$ strengths out to notch sizes of $i_n = 10$, whereas the LLS model and simulations show that the $m = 10$ materials are weaker, particularly for larger notch sizes. This differing behavior can again be traced to fiber pullout. The fiber pullout stress, absent in the Batdorf model, acts as a tremendous stabilizing influence at larger notch sizes and ultimately dominates the notch strength and composite toughness,

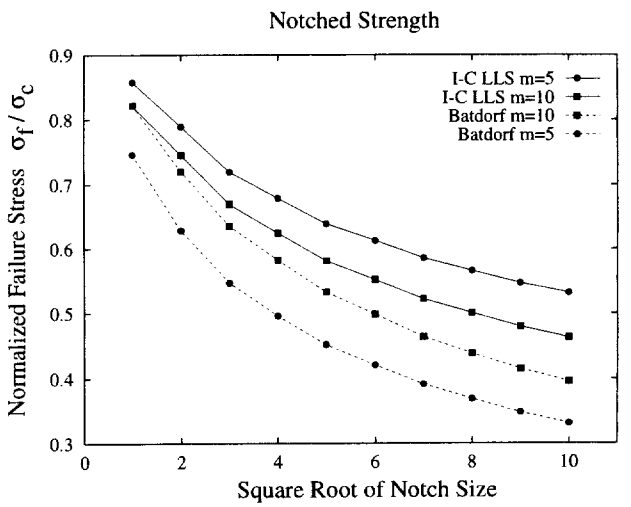

Fig. 3. Normalized fiber bundle notch strength σ_f^*/σ_c vs initial notch size i_n, as predicted by the Batdorf-type model and an LLS analytic model of Ibnabdeljalil and Curtin (IC), for fiber Weibull moduli of 5 and 10. Note that the Batdorf-type model predicts that $m = 5$ is always weaker than $m = 10$, in contrast to the predictions of the LLS model.

as physically expected and observed in Ti-MMCs. Using the Batdorf model for guidance in composite design would thus suggest that high-Weibull fibers are preferable for both high strength and high toughness, which is not really the case. High Weibull fibers provide higher strengths, but do sacrifice toughness, or notch strength, as observed in the LLS model.

Thus, in spite of the reasonable success of the Batdorf-type model in predicting unnotched tensile strength at higher Weibull moduli, it is not very accurate in assessing either the magnitude or trends in notch strength of composites operating under LLS.

6. SUMMARY

We have applied a local load sharing simulation model to predict the ultimate tensile strengths of Ti-1100 metal matrix composites. Utilizing measured constitutive properties, the model predicts strengths in excellent agreement with the measured values with no adjustable parameters. The model is thus predictive, given the as-processed fiber strengths for a particular material. The general model can then be used to assess the sensitivity of composite performance to variations in the constituent properties such as fiber strength and volume fraction, and interfacial sliding resistance. An analytic Batdorf-type model, which is an approximation to the LLS simulation model, shows equally good agreement with the measured results. However, the predictions of the two models are rather different at lower Weibull moduli. The simulation-derived analytic model, which incorporates many sources of fluctuations that can influence strength, such as fiber pullout, appears to be more robust over a range of fiber Weibull moduli. A comparison of predicted notch strength also shows marked difference between the Batdorf-type and simulation-based models.

The LLS strength model, validated by the present detailed comparison to experiment, serves as a clear base for further modeling and understanding of MMC failure. Extensions to incorporate matrix creep behavior, time-dependent interfacial phenomena, and time-dependent fiber strength degradation, are all possible within the framework of the present model. The importance influence of composite size effects can also be understood within the present framework. Some work along these lines for aluminum metal matrix composites is currently being carried out by Ramamurty *et al.* (1997), and shows that the present LLS model predicts quite well the dependence of tensile strength on composite size over a wide range of sizes. The effects of processing fiber damage on composite strength can also be investigated, and toughness (including the important influence of bridging Ti–metal ligaments) can be studied by suitable generalizations of the simulation model. Finally, the effects of spatially heterogeneous fiber distributions, both locally and over longer length scales, can be studied starting from the current model. Analysis of many of these problems will be reported on in our future work.

Acknowledgements—The authors thank both the NSF Science and Technology Center at Virginia Tech. and the Air Force Office of Scientific Research (Grant F49620-95-1-0158) for support of this work.

REFERENCES

Batdorf, S. B. (1982) Tensile strength of unidirectional reinforced composites—I. *Journal of Reinforced Plastic Composites* **1**, 153–164.

Batdorf, S. B. and Ghaffarian, R. (1982) Tensile strength of unidirectional reinforced composites—II. *Journal of Reinforced Plastic Composites* **1**, 165–176.

Beyerlein, I. J. and Phoenix, S. L. (1997) Stress concentrations around multiple fiber breaks in an elastic matrix with local yielding or debonding using quadratic influence superposition. *Journal of Mechanics and Physics of Solids* **44**, 1997–2039.

Cox, B. N., Carter, W. C. and Fleck, N. A. (1994) A binary model of textile composites—I. Formulation. *Acta Metallica Materiala* **42**, 3463–3479.

Curtin, W. A. (1991) Theory of mechanical properties of ceramic–matrix composites. *Journal of American Ceramic Society* **76**, 2837–2845.

Curtin, W. A. and Zhou, S. J. (1995) Influence of processing damage on performance of fiber-reinforced composites. *Journal of Mechanics and Physics of Solids* **43**, 343–363.

Du, Z.-Z. and McMeeking, R. M. (1995) Creep models for metal matrix composites with long brittle fibers. *Acta Metallica Materiala* **43**, 701–726.

Fabeny, B. and Curtin, W. A. (1996) Damage-enhanced creep and rupture in fiber-reinforced composites. *Acta Metallica Materiala* **44,** 3439–3451.

Gundel, D. B. and Wawner, F. E. (1997) Experimental and theoretical assessment of the longitudinal tensile strength of unidirectional SiC fiber/titanium matrix composites. *Composites Science and Technology* **57,** 471–481.

Harlow, D. G. and Phoenix, S. L. (1981) Probability distributions for the strength of composite materials II: a convergent sequence of tight bounds. *International Journal of Fracture* **17,** 601–629.

Hedgepeth, J. M. and van Dyke, P. J. (1967) Local stress concentrations in imperfect filimentary composite materials. *Journal of Composite Materials* **1,** 294–309.

Ibnabdeljalil, M. and Curtin, W. A. (1997a) Strength and reliability of fiber-reinforced composites: localized load-sharing and associated size effects. *International Journal of Solids and Structures* **34,** 2649–2668.

Ibnabdeljalil, M. and Curtin, W. A. (1997b) Strength and reliability of notched fiber-reinforced composites, *Acta Metallica Materiala*, in press.

Iyengar, N. and Curtin, W. A. (1997) Time-dependent failure in fiber-reinforced composites by fiber degradation. *Acta Metallica Materiala* **45,** 1489–1502.

MacKay, R. A., Draper, S. L., Ritter, A. M. and Siemers, P. A. (1991) A comparison of the mechanical properties and microstructures of intermetallic matrix composites fabricated by two different methods. *Metallic Transactions* **25A,** 1443–1455.

Phoenix, S. L., Ibnabdeljalil, M. and Hui, C.-Y. (1997) Size effects in the distribution for strength of brittle matrix composites: analysis and Monte-Carlo simulation. *International Journal of Solids and Structures* **34,** 545–568.

Ramamurty, U., Zok, F. W., Leckie, F. A. and Deve, H. E. (1997) Strength variability in alumina fiber-reinforced aluminum matrix composites. *Acta Materialia* **45,** 4603–4613.

Weber, C. H., Du, Z.-Z. and Zok, F. W. (1996) High temperature deformation and fracture of a fiber reinforced titanium matrix composite. *Acta Materialia* **44,** 683–695.

Xu, J., Cox, B. N., McGlockton, M. A. and Carter, W. C. (1995) A binary model of textile composites—II. The elastic regime. *Acta Metallica Materiala* **43,** 3511–3524.

Zhou, S. J. and Curtin, W. A. (1995) Failure of fiber composites: a lattice Green function model. *Acta Metallica Materiala* **43,** 3093–3104.